

DETERMINATION OF POROSITY AND POROSITY DEVELOPMENT DURING GASIFICATION FROM THERMAL DESORPTION METHODS

L. Zhang and J.M. Calo
Chemical Engineering Program
Division of Engineering
Brown University
Providence, Rhode Island 02912, U.S.A.

Keywords: Char porosity; porosity development; thermal desorption methods.

INTRODUCTION

In the current work, a new approach is explored for the characterization of porosity and porosity development in carbons and chars. It is shown that there exist both qualitative and quantitative relationships between porosity development and post-reaction desorption features of oxygen surface complexes formed during the activation process. It is proposed to exploit these relationships to develop a porosity characterization method based on the interpretation of post-activation temperature programmed desorption (TPD) spectra.

EXPERIMENTAL

The samples used in the experiments were chars produced from Wyodak subbituminous coal obtained from Argonne Premium Coal Sample Bank [1], and from phenol-formaldehyde resin synthesized in our laboratory. The latter material was used as a prototype of a non-mineral matter containing char. The char samples were produced in a tube furnace at 1000°C for 2h in flowing ultrahigh purity helium.

All the oxidation and thermal desorption experiments were carried out in the TPD-MS/TGA apparatus. For gasification, the samples were exposed to one atmosphere of oxygen at a selected temperature, and burned-off to varying extents. The subsequent thermal desorptions were all carried out at a heating rate of 50K/min to 1200°C in ultrahigh purity helium carrier gas, without exposing the previously oxidized samples to ambient air.

Adsorption isotherms for all the char samples were obtained using a Quantachrome Quantasorb surface area analyzer with nitrogen at 77K.

RESULTS AND DISCUSSION

Char Characterization. The total specific surface area, external surface area, and micropore volume of the samples were determined from the nitrogen isotherm data using the so-called α_s -plot method [2]. This technique is based on a comparison of the shape of the adsorption isotherm of a sample with that of a standard nonporous reference material. The α_s -plot method consists of plotting adsorption normalized to a particular point (typically $p/p^\circ = 0.4$; i.e., $\alpha_s = n/n_{0.4}$) for the reference material vs. p/p° to obtain a standard α_s curve. This curve is then used to construct the α_s -plot from the isotherm of the test sample. The slope of the resultant plot at low α_s provides the total surface area; the slope of the upper linear branch gives the nonmicroporous surface area; and the extrapolation of this branch of the curve to $\alpha_s = 0$ provides the total micropore volume. α_s -plots were constructed for all the nitrogen adsorption isotherms for the current samples using data for the standard nonporous carbon proposed by Rodriguez-Reinoso *et al.* [3]. Corresponding surface areas and pore volumes were also obtained via comparison with the isotherm for the reference adsorbent given in this reference [3], following the data work-up procedures contained therein.

Wyodak Coal Char. Figures 1 and 2 present the thermal desorption spectra for the Wyodak coal char samples as a function of burn-off. In Figures 3 and 4 the total evolved CO and CO₂ obtained from these figures are compared to the micropore volume and the nonmicroporous surface area, respectively, as determined from the α_s -plots, as described above. It is noted that the CO evolution was "corrected" by subtraction of the CO₂ signal, which is explained subsequently. The nitrogen adsorption data indicate that the total surface area (not shown), the nonmicroporous surface area, and the micropore volume all initially increase with burn-off, pass through maxima around 40% burn-off, and decrease steadily thereafter. This behavior is quite typical of carbonaceous materials [4]. As the burn-off proceeds, the nonmicroporous (i.e., the larger porosity) surface area increases continuously but more rapidly prior to 40% burn-off, and less rapidly at higher degrees of burn-off, as shown in Figure 4. This behavior indicates that the microporosity continues to develop up to about 40% burn-off, and decreases thereafter; while, the larger porosity develops continuously with burn-off. These results are consistent with the classical picture of microporosity development at low conversions, followed by pore wall collapse and concomitant surface area loss at higher conversions [5]. The principal point of these figures, however, is that the CO and CO₂ evolution correlate quite well with the micropore volume and the nonmicroporous surface area, respectively.

Resin Char. Summaries of the corresponding data for resin char are presented in Figures 5 and 6. As shown, this char behaves somewhat differently than the Wyodak coal char. The nitrogen adsorption data indicate that the micropore volume increases to a maximum at about 45% burn-off, and decreases thereafter. The nonmicroporous surface area, however, increases steadily and monotonically up to 72% burn-off. It is noted that even though the larger porosity increases with extent of burn-off, the majority of the porosity is still microporous over the entire activation

process. That is, even at 72% burn-off, the surface area contribution from the larger porosity is only about 5% of the total surface area. In any case, as for the Wyodak coal char, the CO and CO₂ evolution correlate quite well with the micropore volume and the nonmicroporous surface area, respectively, in spite of the fact that the CO and CO₂ TPD spectra for resin char (not shown) differ considerably from the Wyodak char spectra, both qualitatively and quantitatively.

Starsinic *et al.* [6] identified carboxylic acid groups on oxidized carbon surfaces using FTIR spectroscopy, and noted that their concentration increases with extent of burn-off. Otake and Jenkins [7] have shown that the CO₂ complexes present on an air-oxidized char are responsible for the acidic nature of the surface, and that the high temperature CO₂ evolution is primarily due to the thermal decomposition of carboxylic acid anhydride surface complexes. Zhuang *et al.* [8] have also found that CO₂ evolution arises from the decomposition of lactone and/or acid anhydride complexes, whereas CO desorption is mainly from carbonyl and ether type complexes. In a DRIFTS study of the formation of surface groups on carbon by oxygen, Fanning and Vannice [9] also reported that initial exposure to oxygen produces ether structures, and that additional exposure develops cyclic anhydride groups.

Apparently, just like nitrogen, which penetrates practically all the char porosity (i.e., micro-, meso- and macroporosity) during adsorption measurements, oxygen can also penetrate all the porosity under gasification conditions to form surface complexes over the entire carbon surface. The obvious conclusion that one can draw from the results presented here is that CO evolution occurs from the entire apparent specific surface area, but that most of the CO₂-evolving surface complexes are formed only on the surfaces of the larger porosity. In a study of the effect of nonreacting gases on the desorption of reaction-created surface complexes on carbon, Britten *et al.* [10] concluded that surface transport processes were involved in the desorption of CO, but that no influence of the nonreactive gases on the CO₂ desorption rate was observed. These results support the conclusion that the CO₂-evolving surface complexes are formed on the surface area in the larger porosity.

From the preceding, it is possible that a large portion of the CO₂ evolution derives from carboxylic acid anhydride complexes. Since the stoichiometry for the thermal decomposition of these groups result in one CO₂ and one CO molecule, the CO evolution was "corrected" by subtracting the CO₂ evolution to account for the CO arising from carboxylic acid anhydride complexes. These are the "corrected" CO values which are plotted in Figures 3 and 5. In both cases, this correction improves the correlation between micropore volume and CO evolution. Therefore, it is concluded that there is some justification to this "correction."

Random Pore Model. In addition to the CO and CO₂ evolution data and the nitrogen adsorption data, the reactivities of the samples as a function of burn-off were also obtained. These latter data were used in conjunction with a random pore model [11] to determine the evolution of the microporosity.

According to the random pore model [11], the sample burn-off, x_c , vs. time, t , follows the relationship:

$$[1/4\pi(1-x_c)dx_c/dt]^2 = A_0 \ln[1/(1-x_c)] + A_1^2 \quad [1]$$

where $A_0 = B_0 v^2/(2\pi)$, and $A_1^2 = (B_1 v)^2$, and B_0 and B_1 are the zeroth and first order moments of the pore number density function, and v is the velocity with which a pore surface element recedes due to reaction. A_0 and A_1 were determined by least squares regression from plots of Eq. [1] derived from the reactivity data. From these values and the surface area at one point (e.g., 5% burn-off), the parameters B_0 , B_1 , and v were obtained. The apparent total specific surface area, S , was then determined from:

$$S = 4\pi(1-\epsilon_{T0})(B_0 v t + B_1) (1-x_c(t)), \quad [2]$$

where ϵ_{T0} is the initial (i.e., zero burn-off) total void fraction. Comparisons of surface areas obtained from the nitrogen BET data with values calculated from Eq. [2] show very good agreement for both chars.

As indicated by the nitrogen adsorption data, both the resin and the Wyodak coal chars are essentially microporous materials at zero burn-off. A Gaussian pore number distribution for the micropore volume was assumed, following Dubinin *et al.* [12]. It was also assumed, as in the original random pore model development, that the probability density function of pore numbers does not vary with burn-off. With these assumptions, the following relationships were derived:

$$(1-\epsilon_{\text{micro}})/(1-\epsilon_{\text{micro}})_0 = \exp[-2\pi(B_0(\Delta r)^2 + 2B_1\Delta r)] \quad [3]$$

$$S_{\text{micro}} = d(\epsilon_{\text{micro}})/d(\Delta r) = 4\pi(1-\epsilon_{\text{micro}})(B_0\Delta r + B_1) \quad [4]$$

where ϵ_{micro} is the void fraction of the micropores, and Δr is the mean micropore radius change.

For the current data, the micropore void fractions, ϵ_{micro} , for the two chars as a function of burn-off were determined from nitrogen adsorption data. The mean micropore radius change, Δr , was then determined from Eq. [3], and the total apparent micropore surface area, S_{micro} , was

determined from Eq. [4]. The difference between total surface area and micropore surface area was taken as the nonmicroporous surface area. The agreement between the nonmicroporous surface areas determined in this manner with those obtained from the α_s -plots was quite good, thereby validating this general approach.

Figure 7 shows the results for the mean micropore radius as a function of burn-off for resin and Wyodak coal chars, as determined using this approach. Here the initial mean micropore radius (i.e., prior to gasification) was determined from the zero burn-off nitrogen adsorption data assuming a normal micropore volume distribution. The resultant mean pore radius prior to oxidation was 1.04 nm for Wyodak coal char, and 0.64 nm for resin char. The variance of the normal distribution was 0.24 nm for Wyodak coal char, and 0.18 nm for resin char. These results indicate that the pore size is larger, and the pore distribution is broader for Wyodak coal char than for resin char prior to activation. It is noted that the rate of mean micropore radius decrease with burn-off at high conversion is slower for resin char than for Wyodak coal char. This suggests that the resin char remains more microporous with burn-off. This conclusion is also apparent from the nonmicroporous surface areas for both chars. From these results, it is concluded that the random pore model theory is capable of providing reasonable predictions of microporosity development during gasification for both resin char and Wyodak coal char.

SUMMARY AND CONCLUSIONS

It is concluded that CO-evolving surface complexes are formed over the entire surface area of all the porosity of the two very different chars investigated, and that the total CO evolution upon thermal desorption is well correlated with the total surface area. It is also concluded that the CO evolution "corrected" for the expected contribution from carboxylic acid anhydride surface complexes is well correlated with the microporosity. It is hypothesized that if these observations can be generalized and calibrated, they could be developed into a new method for the characterization of char porosity, in conjunction with the "extended" random pore model.

ACKNOWLEDGEMENT

This work was supported by Grant No. DE-FG22-91PC91305 from the UCR Program of the U.S. Department of Energy.

REFERENCES

1. Vorres, K.S., Users Handbook for the Argonne Premium Coal Samples, ANL/PCSP-93/1, DOE, Argonne, IL, 1993.
2. Gregg, S.J., and Sing, K.S.W., Adsorption, Surface Area, and Porosity, 2nd ed., Academic Press, NY, 1982.
3. Rodriguez-Reinoso, F., Martin-Martinez, J.M., Prado-Burguete, C., and McEnaney, B., *J. Phys. Chem.* **91**, 515 (1987).
4. Walker, P.L. Jr., in *Carbon and Coal Gasification*, Figueiredo, Moulijn, eds., NATO ASI Series, 9.3, 1986.
5. Miura, K. and Hashimoto, K., *IEC Proc. Des. Dev.* **23**, 138-145, 1984.
6. Starsinic, M., Taylor, R.L., Walker, P.L., Jr., and Painter, P.C., *Carbon* **21**, 69 (1983).
7. Otake, Y. and Jenkins, R.G., *Carbon* **31**, 109 (1993).
8. Zhuang, Q-L, Kyotani, T., Tomita, A., *Energy and Fuels* **8**, 714, 1994.
9. Fanning, P.E. and Vannice, M.A., *Carbon* **31**, 5, 721, (1993).
10. Britten, J. A., Falconer, J. L. and Brown, L. F., *Carbon* **23**, 627 (1985).
11. Gavalas, G. *AIChE J.* **36**, 577 (1980).
12. Dubinin, M. M., *Chemistry and Physics of Carbon*, Vol. 2, Academic, NY, p. 51 (1966).

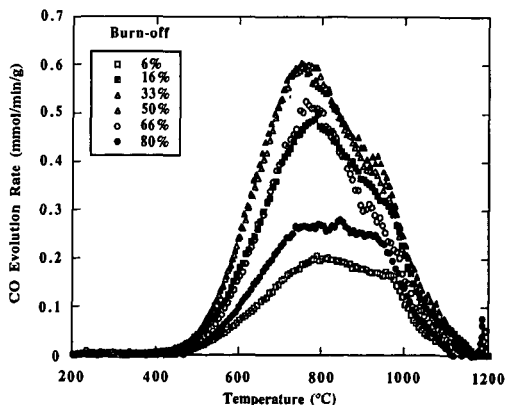


Figure 1. 50K/min CO TPD spectra from Wyodak char as a function of burn-off in oxygen

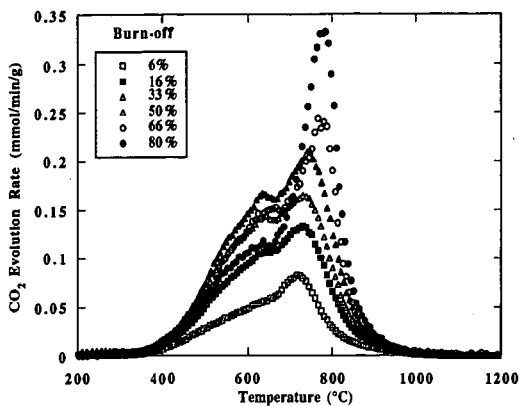


Figure 2. 50K/min CO₂ TPD spectra from Wyodak char as a function of burn-off in oxygen (0.1MPa, 420°C).

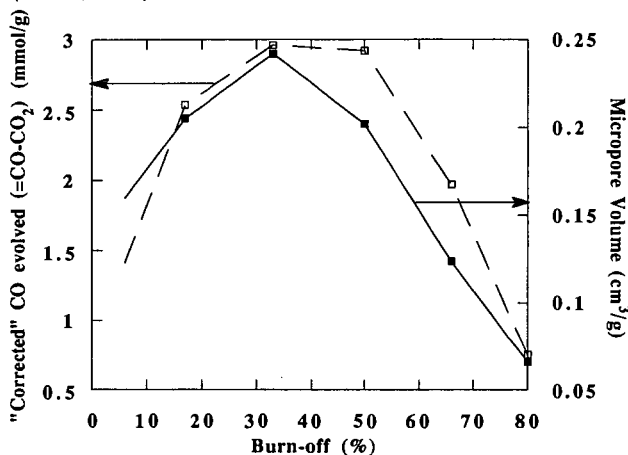


Figure 3. Comparison of total "corrected" CO evolved with micropore volume for Wyodak coal char as a function of burn-off (0.1MPa, 420°C).

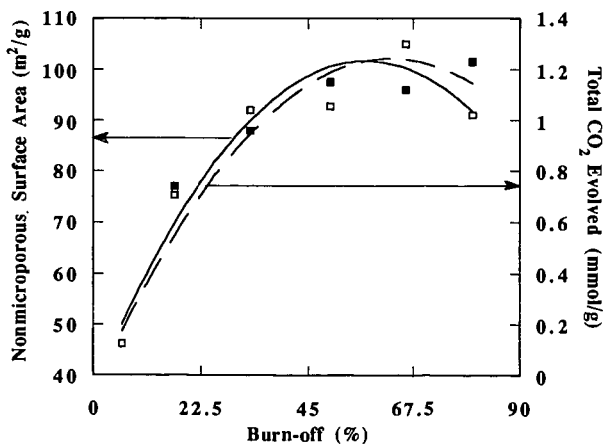


Figure 4. Comparison of total CO₂ evolved with nonmicroporous surface area as a function of burn-off (0.1MPa, 420°C).

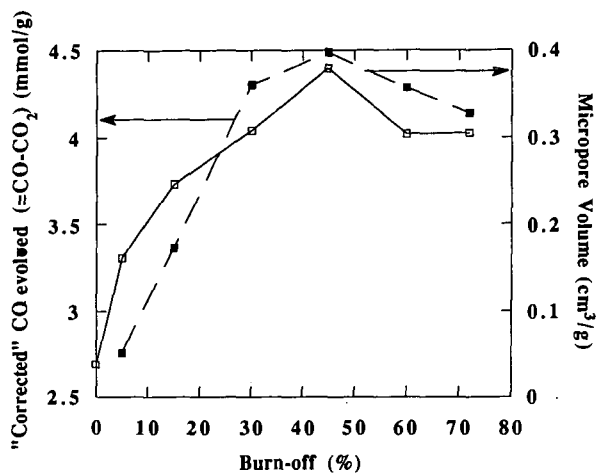


Figure 5. Comparison of total "corrected" CO evolved with micropore volume for resin char as a function of burn-off (0.1 MPa, 470°C).

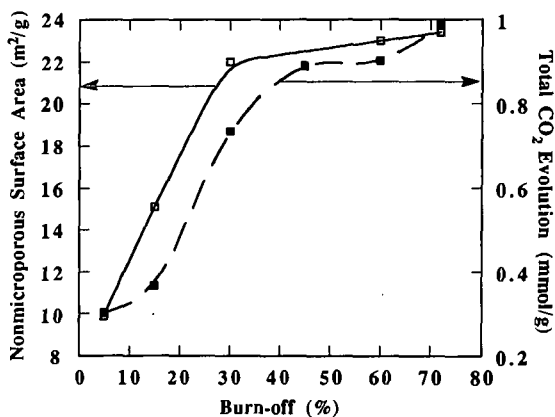


Figure 6. Comparison of total CO₂ evolved with nonmicroporous surface area for resin char as a function of burn-off (0.1 MPa, 470°C).

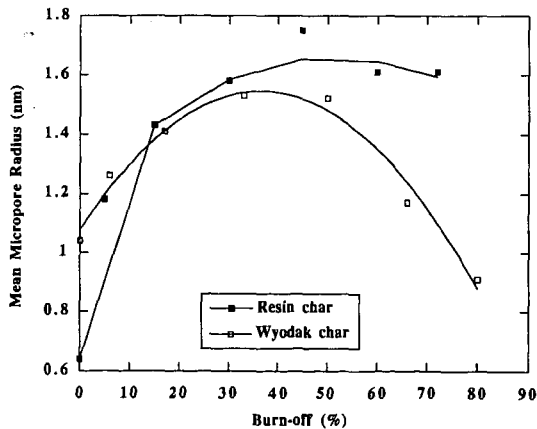


Figure 7. Mean pore radius as a function of burn-off for resin and Wyodak coal char, as determined from the "extended" random pore model.